Water Research 202 (2021) 117404

Contents lists available at ScienceDirect

Water Research

journal homepage: www.elsevier.com/locate/watres

Anoxic storage to promote arsenic removal with groundwater-native iron

Md Annaduzzaman [a,*], Luuk C. Rietveld [a], Devanita Ghosh [b], Bilqis A. Hoque [c], Doris van Halem [a]

[a] Sanitary Engineering Section, Water Management Department, Delft University of Technology, the Netherlands
[b] Laboratory of Biogeochem-mystery, Centre for Earth Sciences, Indian Institute of Science, Bangalore, India
[c] Environment and Population Research Centre, Dhaka, Bangladesh

ARTICLE INFO

Keywords:
Groundwater
Treatment
Anoxic
Storage container
Arsenic
Iron

ABSTRACT

Storage containers are usually used to provide a constant water head in decentralized, community groundwater treatment systems for the removal of iron (Fe) and arsenic (As). However, the commonly practiced aeration prior to storage assists in rapid and complete Fe^{2+} oxidation, resulting in poor As removal, despite sufficient native-Fe^{2+} in the source water. In this study, it was found that application of anoxic storage enhanced As removal from groundwater, containing ≥300 μg/L of As(III) and 2.33 mg/L of Fe^{2+} in an As affected village of Rajshahi district in Bangladesh. Although the oxidation of Fe^{2+} and As(III) during oxic storage was considerably faster, the As/Fe removal ratio was higher during anoxic storage (61–80±5 μgAs/mgFe) compared to the oxic storage (45±5 μgAs/mgFe). This higher As removal efficacy in anoxic storage containers could not be attributed to the speciation of As, since As(V) concentrations were higher during oxic storage due to more favorable abiotic (As(III) oxidation by O_2 and Fenton-like intermediates) and biotic (As(III) oxidizing bacteria, e.g., *Sideroxydans, Gallionella, Hydrogenophaga)* conditions. The continuous, in-situ hydrous ferric oxide floc formation during flow-through operation, and the favorable lower pH aiding higher sorption capacities for the gradually formed As (V) likely contributed to the improved performance in the anoxic storage containers.

1. Introduction

The geogenic groundwater contamination of arsenic (As) negatively affects the quality of drinking water, leading to health risks in many countries including Bangladesh and India (Chakraborty et al., 2015; Smedley and Kinniburgh, 2002). Long-term consumption of As contaminated water may cause skin lesions, melanosis, hyperkeratosis, skin cancer and internal organs damage (Farmer and Johnson, 1990; Guo et al., 2013; Li et al., 2012; Luzi et al., 2004). According to the World Health Organization (WHO), the recommended values for As in drinking water should not exceed 10 μg/L (WHO, 2011), whereas 50 μg/L is the maximum allowable limit in Bangladesh. However, As can be found in groundwater-based drinking water supplies in Bangladesh up to several mg/L (Nordstrom, 2002). In oxidizing conditions and circumneutral pH, such as in surface waters, arsenate [As(V)] is the predominant species, which is usually present in the immobile state, forming oxyanions ($H_2AsO_4^-$, $HAsO_4^{2-}$) (Katsoyiannis and Zouboulis, 2004; Lafferty et al., 2010). However, under circumneutral pH and reducing conditions like in groundwater aquifers, arsenite [As(III)] specie is the more toxic, mobile, and thermodynamically stable in the non-ionic form (H_3AsO_3) (Villalobos et al., 2014). Therefore, pre-oxidation from As(III) to As(V) is an essential step for As contaminated water treatment processes such as precipitation, co-precipitation, coagulation-filtration, and adsorption on iron (Fe)-oxides, activated alumina or bone char (Bai et al., 2016; Begum et al., 2016; Niazi et al., 2018; Pio et al., 2015; Zhang et al., 2010). However, oxidation of As(III) through dissolved oxygen (DO) is thermodynamically feasible but is slow (Gude et al., 2018b; Sorlini and Gialdini, 2010).

Aeration is commonly used for oxidizing Fe^{2+} and removing carbon dioxide, methane, hydrogen sulfide, and volatile organic compounds from water (Bruins et al., 2014; Katsoyiannis et al., 2008; Vries et al., 2017). Moreover, if the water source also contains As, the oxidation of Fe^{2+} can also enhance As(III) oxidation by reactive oxidation species (ROS) and/or Fenton-like chemical reactions (Hug et al., 2001; Hug and Leupin, 2003; Roberts et al., 2004). The freshly formed hydrous ferric oxide (HFO) flocs from Fe^{2+} oxidation can bind and co-precipitate with As (Katsoyiannis et al., 2015; Roberts et al., 2004; Senn et al., 2018), where the binding-affinity for As(V) is stronger than for As(III) (Bissen and Frimmel, 2003; Cui et al., 2018). However, the removal of As with oxidized HFO flocs has been found to be inefficient due to rapid and

* Corresponding author.
E-mail address: M.Annaduzzaman@tudelft.nl (M. Annaduzzaman).

https://doi.org/10.1016/j.watres.2021.117404
Received 10 February 2021; Received in revised form 18 June 2021; Accepted 29 June 2021
Available online 5 July 2021

almost complete Fe^{2+} oxidation during storage or filtration before complete As(III) oxidation (Annaduzzaman et al., 2021; Gude et al., 2016; Roberts et al., 2004). Moreover, as formerly observed, the rise in pH during aeration increases the negative surface charge on HFO flocs and hence decreases As removal potential (Dixit and Hering, 2003; Han et al., 2016).

Storage containers are usually used to provide a constant water head in decentralized, community treatment systems for the removal of iron (Fe) and arsenic (As) (Chakraborty et al., 2016). However, the commonly practiced aeration prior to storage results in rapid and complete Fe^{2+} oxidation, resulting in poor As removal despite sufficient native-Fe^{2+} in the source water. As a result, the conventional oxic storage and filtration processes require additional chemical oxidants/adsorbents for As removal. In a recent study (Annaduzzaman et al., 2021), it was found that delayed aeration before sand filtration enhanced overall As removal. It is hypothesized that the observed partial Fe^{2+} oxidation during anoxic storage promoted As removal in the following aeration-filtration steps. However, the oxidation mechanisms and effects of temporal changes in various water quality parameters in such storage containers are not yet fully understood. Therefore, this study aims to address the following knowledge gaps: (i) the mode of Fe^{2+} and As(III) oxidation, being either homogeneous, heterogeneous (surface-related process), biological, or in various combinations (van Beek et al., 2015; Vries et al., 2017), (ii) the role of various biological processes by subsurface-derived indigenous microorganisms (Crognale et al., 2019; Gude et al., 2018a), and (iii) the effect of a larger surface area to adhere biofilms by application of bio-carriers in the storage container.

Thus, this novel concept of anoxic storage was monitored to understand the oxidation processes of groundwater native-Fe^{2+} and As(III), and their effect on As removal, compared to the conventional oxic storage in the presence and absence of bio-carriers. The oxic and anoxic storage container experiments were conducted over 30 days with natural groundwater, in the presence of native-Fe^{2+} (2.33 mg/L), As (>300 µg/L), and other con-t-a-m-i-nants like PO_4^{3-} (2.15 mg/L) and NH_4^+ (0.96 mg/L). Furthermore, this research also studied the role of bio-carriers and consequent changes in bacterial growth in the storage containers.

2. Materials and methods

2.1. Groundwater sample quality

The experiments were performed in polypropylene storage containers (GAZI, Bangladesh) with a capacity of 75 L, using As contaminated groundwater in the affected Uttar Kazirpara village in Paba, Rajshahi district, Bangladesh. The relevant water composition of the used groundwater is shown in Table 1. The anoxic groundwater was extracted from a borehole of 50±1 m depth using a submersible pump (GAZI, Bangladesh).

Table 1
The relevant groundwater compositions used in the study.

Water Quality Parameters	Unit	Raw Groundwater
pH	[-]	6.94
Dissolved Oxygen (DO)	mg/L	0.07*
Oxygen Reduction Potential (ORP)	mV	−110±10
Electrical Conductivity (EC)	µS/cm	675
Temperature	°C	26.7
As(total)	µg/L	329±3%
As(V)	µg/L	39±5%
As(III)	µg/L	290±5%
Fe^{2+}	mg/L	2.33±3%
Manganese (Mn)	µg/L	600±5%
Ammonium (NH_4^+)	mg/L	0.96±0.02(SD)
Nitrate (NO_3^-)	mg/L	0.39±0.02(SD)
Phosphate (PO_4^{3-})	mg/L	2.15±0.03 (SD)

* The observed DO value is the lower limit of the measuring device.

2.2. Experimental set-up of storage containers

The experimental set-up consisted of eight 75 L polypropylene containers (GAZI, Bangladesh) to study four storage conditions in duplicate, namely, oxic (with/without bio-carriers) and anoxic (with/without bio-carriers) (Fig. 1). The containers with bio-carriers were half-filled with AnoxKaldnes K3 shaped bio-carriers, purchased from a local shop in Dhaka (OSMOSIA Water), Bangladesh (Fig. 1). To ensure an abiotic environment at the start of the experiments, the containers were thoroughly sterilized with 35% (w/w) hydrogen peroxide (H_2O_2) (Sigma-Aldrich). Every 24 h, the stored water was replaced with freshly extracted groundwater without removing the precipitated Fe-oxide sludge. This refill process was chosen to replicate the conventional storage practices, where the precipitated Fe-oxide sludge generally accumulates in the storage container for several weeks. The groundwater was aerated by passing it through a showerhead, placed 35 cm above the top of the containers with oxic storage. In the containers with anoxic storage, the inlet of the extracted groundwater was filled without aeration from the bottom of the containers. The anoxic containers were overflown for an additional five minutes to avoid any incidental aeration of water. The water sampling was performed every 60 min for the first eight hours on days 1, 5, 10, 20, and 30 of the experimental period. The experimental time of eight hours was selected to prevent full emptying of the storage container (max ±90%) and consequent discontinuation of the column feed.

During each sampling event, the pH, dissolved oxygen (DO), oxygen reduction potential (ORP), and temperature (T) were directly measured on-site. In the course of each sampling time, 15 mL water samples (both 0.45 µm (VWR) filtered and unfiltered) were collected in polypropylene transparent 15 mL centrifuge tube (Sigma Aldrich) and acidified with ultrapure HNO_3 acid (ACS reagent, 70%; Formula weight 60.01 g/mol; Sigma Aldrich) to make up for 1.5% acidification of the solutions to preserve for elemental quantification (such as Fe, As, etc.). The water sample was collected using a 60 mL syringe and pre-fixed sampling tube (IV injection tube, SQUARE, Bangladesh) at approximately 10 cm above the bottom of the container (Fig. 1). This arrangement was used to avoid opening of the container's lids, risk of aeration during water sampling and to maintain consistency of sample quality. Additionally, three times a day (0, 4, and 8 h), 250 mL filtered (0.45 µm) water samples (without acidification) were collected in the 250 mL polypropylene laboratory-grade water vials for ammonium (NH_4^+), nitrate (NO_3^-), and phosphate (PO_4^{3-}) analyses. The used chemicals, instruments and reagents during this pilot-scale study are detailed in supplementary data (Table S1), where Fig. S1 represents the experimental approach with relevant parameters in the respective steps. All sample collections and parameter measurements were performed in duplicate from each container.

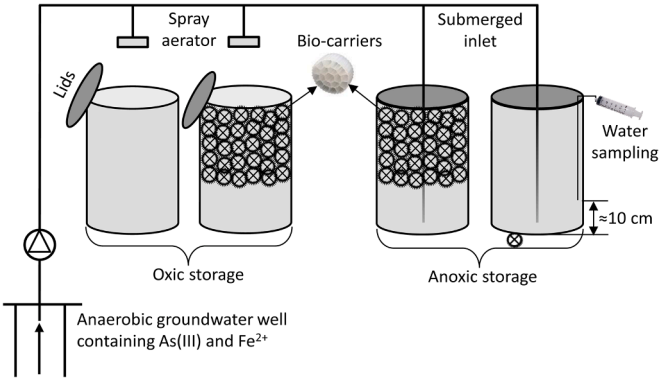

Fig. 1. Schematic overview of the experimental storage container set-up with oxic (left) and anoxic (right) storage conditions. Half of the containers were filled with bio-carriers and all container settings were constructed in duplicate.

2.3. Chemical analyses

The pH, DO, ORP, and T were directly measured in the field using WTW electrodes (SenTix 940, FDO®925, SenTix ORP 900, and TerraCon 925, respectively) and calibrated using standard method before use. The measurement consistency was maintained by placing the WTW electrodes at ±10 cm above the bottom of the container. All sample collections and parameter measurements were performed in duplicate from each container. Elemental analysis was carried out by Inductively Coupled Plasma Mass Spectrometry, ICP-MS (Alanlytik Jena model PlasmaQuant MS) at Delft University of Technology, the Netherlands. Other ions such as NH_4^+, NO_3^-, and PO_4^{3-} were quantified at Rajshahi Regional Laboratory, Department of Public Health Engineering (DPHE), Bangladesh.

2.4. Arsenic speciation

For the As speciation, the ion-exchange resin Amberlite® IRA-400 chlorite was used. This speciation was performed by a 60 mL syringe with 30 mL ion-exchange resin. After 0.45 μm filtration, 100 mL sample were passed through 30 mL ion-exchange resin column. The remaining As concentration in the resin filtrate was considered as reduced As(III) species (Gude et al., 2016; Karori et al., 2006). Finally, the obtained As (III) species level from the resin filtrate was subtracted from 0.45 μm filtrate (total) As concentration to determine dissolved As(V).

2.5. Microbial sampling and analyses

For the microbial community profiling, the biomass from the container wall (inside) and bio-carriers were collected and stored at −80 °C. From these samples, around 0.25 g was used for DNA extraction using the DNeasy UltraClean microbial kit (Qiagen) at Department of Biochemistry and Molecular Biology, Rajshahi University, Bangladesh. Afterward, the DNA samples were used for metagenomics analysis at Novogene Hongkong, China. The cetyl-trimethylammonium bromide/sodium dodecyl sulfate (CTAB/SDS) method was used to extract total environmental DNA from the samples. The purity and concentration of the DNA were examined on 1% agarose gel horizontal electrophoresis. The environmental DNA samples were used for metagenomics analysis with further dilution to 1 ng/μL and amplification of the V3 region of 16S rRNA genes were performed using the universal primers 341F (5′-CCT ACG CGA GGC AGC AG −3′) and 517r (5′- ATT ACC GCG GCT GCT GG −3′) (Muyzer et al., 1993) at Novogene Hongkong, China. Polymerase chain reactions (PCR) were performed with Phusion® High-Fidelity PCR Master Mix (New England Biolabs). The same volume of 1X loading buffer was mixed (containing SYBR green) with PCR products and electrophoresis on 2% agarose gel electrophoresis was performed for detection. Samples with a bright prominent band strip between size 400–450 bp were chosen for further experiments. The PCR products were mixed in equal ratios and purified with the Qiagen Gel Extraction Kit (Qiagen, Germany). The Illumina HiSeq paired-end raw reads were generated with NEBNext® UltraTM DNA Library Prep Kit and quantified via Qubit and qPCR.

The Illumina HiSeq paired-end raw reads were checked for quality (Base quality, base composition, GC content) using the FastQC tool (Andrews et al., 2010). The QIIME (Version: 1.9.1) pipeline (Caporaso et al., 2010) was used for the selection of 16S RNA, clustering, and OTU picking followed by taxonomic classification based on the SILVA database and statistical analysis. The chimeric sequences were removed from the libraries using the de-novo chimera removal method UCHIME implemented in the tool VSEARCH. Pre-processed reads from all samples were pooled and clustered into Operational Taxonomic Units (OTUs), based on their sequence similarity using the Uclust program (similarity cutoff = 0.97). A representative sequence was identified for each OTU and aligned against the SILVA core set of sequences using the PyNAST program (Caporaso et al., 2010). The representative sequences of the OTUs were also used to predict KEGG orthodoxy (KO) abundances using PICRUSt2 (Langille et al., 2013) and microbial pathways were inferred. The six metagenomic library datasets from the containers under oxic (S1, S2, S3) and anoxic (S1, S2, S3) conditions were clustered, based on the arithmetic mean of weighted Unifrac distance using Unweighted Pair Group Method (UPGMA). An unrooted Neighbor-Joining (NJ) tree of the 35 predominant and common bacterial 16S rRNA sequences was build using the software MEGA X version 10.1. The raw sequencing data have been submitted to the NCBI Sequence Read Archive; accession number PRJNA673456 (https://www.ncbi.nlm.nih.gov/sra/PRJNA673456).

3. Results and discussion

3.1. Immediate changes in pH, DO, ORP and Fe^{2+}

The pH, ORP, DO, and Fe^{2+} concentration during oxic and anoxic storage without the presence of bio-carriers, measured at the start of the experiment (day 1), are shown in Fig. 2. While the natural groundwater pH, DO, and ORP were 6.94, 0.07 mg/L, and −110 mV, respectively, after aeration the average pH, DO, and ORP increased to 7.5(±0.03), 6.75(±0.05) mg/L, and 130(±10) mV, respectively. This was due to atmospheric gaseous exchange resulting in the release of CO_2 and uptake of O_2. The results for the containers with bio-carriers are shown in Supplementary Fig. S2. During the 8 h of observation, the pH and ORP remained stable during oxic storage (Fig. 2a,c, and S2a,c), and DO remained above 6.26 mg/L (Fig. 2b, S2b). The dissolved Fe concentration (considered as Fe^{2+}) dropped to an average of 0.30 mg/L from its initial (groundwater) concentration of 2.33 mg/L, which was due to rapid Fe^{2+} oxidation at the high DO and pH ($t_{1/2}$: roughly 2–3 min; Fig. 2d) (Morgan and Lahav, 2007; Stumm and Lee, 1961).

During anoxic storage Fe^{2+} oxidation was slow in comparison with the oxidation rate during oxic storage, due to the lower levels of pH (6.9), DO (0.35 mg/L), and ORP (±−100 mV) (Fig. 2a,b,c), as evidenced during earlier studies (Vollrath et al., 2012; Wang et al., 2013). The ORP remained stable, similar to its initial value (±−110 mV) over 8 h (Fig. 2c), while DO dropped from 0.35 mg/L to 0.23 mg/L. After the experimental 8 h, 1.39(±0.05) mg/L of Fe^{2+} remained dissolved in the anoxic stored water (Fig. 2d, S2d). The observed 0.94 mg/L of Fe^{2+} oxidation during anoxic storage corresponded to the average consumed 0.13 mg/L of DO, which was equal to the DO drop over 8 h. Part of the Fe^{2+} (0.40 mg/L) oxidized immediately during the filling of the containers, as minor DO intrusion could not be avoided upon filling the container. In the first 24 h of the experiments, no or negligible biological growth and metabolic processes could be expected, thus abiotic Fe^{2+} oxidation must have been predominated, where DO acted as an electron-acceptor in both storage conditions.

3.2. Immediate changes in As(III) oxidation and removal

Under both oxic and anoxic conditions, As(III) oxidation started immediately upon filling of the containers ($t = 0$) and continued over the observed experimental period of 8 h, as shown in Fig. 3. At the start of the experiment, 100 μg/L and 55 μg/L of As(III) was oxidized during oxic and anoxic storage, respectively. Over the next 8 h, an additional 48% As (III) oxidation (from 188 μg/L to 97 μg/L) was detected in the oxic storage (Fig. 3a), whereas in the anoxic storage only 22% (from 236 μg/L to 183 μg/L) additional As(III) oxidation (Fig. 3b) was observed. As a result, the dissolved As(V) concentration increased in both storage conditions.

During oxic storage, As(III) oxidation was faster than in the anoxic storage, probably due to the oxidation of 2.03 mg/L Fe^{2+}, which is known to result in reactive intermediate species (Ciardelli et al., 2008; Cui et al., 2018; Leupin and Hug, 2005; Tian et al., 2017). After almost complete oxidation of Fe^{2+} (2.03 mg/L) in oxic storage (after 5 min), the oxidation of As(III) slowed down to a rate of 11 μg/L/h, probably due to

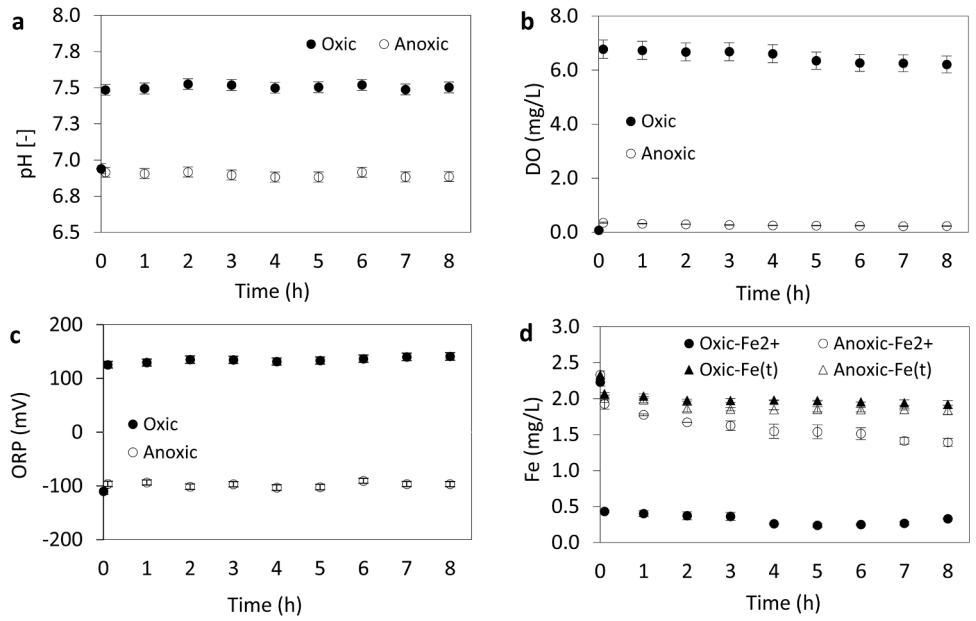

Fig. 2. Physicochemical parameters during the first 24 h of the experiment during oxic and anoxic storage containers without bio-carriers (a) pH, (b) DO, (c) ORP changes, and (d) physicochemical parameters as a function of Fe^{2+} concentration. The error bars represent the standard deviations.

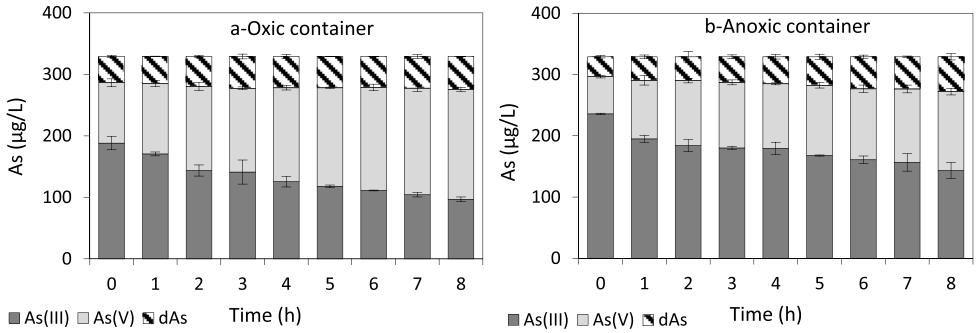

Fig. 3. Arsenic speciation during (a) oxic and (b) anoxic storage containers without bio-carriers over a period of 8 h on the first experimental day. The error bars represent the standard deviations.

homogeneous oxidation with O_2 (DO >6.3 mg/L) (Lowry and Lowry, 2002; Shafiquzzaman et al., 2011), which was in the same order of magnitude as the homogeneous As(III) oxidation observed by Shumlas et al. (2016). The oxidation of As(III) under anoxic conditions was slow (6.5 µg/L/h). The limited concentrations of DO in the anoxic containers resulted in partial/slow Fe^{2+} oxidation and, consequently, the coexistence of Fe^{2+} and oxidized Fe (HFO flocs) stimulated heterogeneous As (III) oxidation (Amstaetter et al., 2010; Tian et al., 2017; Wang and Giammar, 2015).

Although the overall removal of As was higher under oxic conditions, the ratio between the removed As and oxidized Fe was higher under anoxic conditions (61 µgAs/mgFe) than under oxic conditions (26 µgAs/mgFe). This result is in-line with earlier studies, indicating that step-wise Fe^{2+} oxidation and precipitation improved As removal by adsorption and/or co-precipitation (Annaduzzaman et al., 2021; Casentini et al., 2016; Roberts et al., 2004). It appears that the freshly formed HFO flocs in the anoxic storage containers were more efficient for As removal under low pH (6.9), compared to the pre-formed HFO and high pH (7.5) during oxic storage (Kim and Nriagu, 2000; Mercer and Tobiason, 2008; Senn et al., 2018). The As(III) oxidation results for storage containers with bio-carriers was similar to the experiments conducted without bio-carriers, both for the oxic and anoxic conditions (Fig. 3, S3). This observation underlines that on the first experimental day, surface-related biological processes did not contribute to the As(III) conversion, and As(III) oxidation could be considered as abiotic.

3.3. *Effect of long-term operation on Fe^{2+} oxidation*

The changes in ORP and Fe^{2+} concentration for the various containers over the experimental period of 30 days are shown in Fig. 4. Throughout the experimental periods, the Fe^{2+} concentration during oxic conditions remained low and constant at 0.2(±0.05) mg/L, and ORP values remained constant too, at 130(±10) mV (Fig. 4a). However, during anoxic storage, both in the presence and absence of bio-carriers, ORP, and Fe^{2+} oxidation increased gradually over the 30 days (Fig. 4c, d). Where in the anoxic storage containers without bio-carriers, on the first day, the ORP remained stable over 8 h, the ORP drifted from −100 mV to −46 mV and from −23 mV to 49 mV on days 5 and 30, respectively (Fig. 4c). During anoxic storage, in the presence of bio-carriers, the ORP drifted from −110 mV on day 1 to −15 mV and −18 mV on days 5 and 30 correspondingly (Fig. 4d). The detected increase in ORP over time during anoxic storage might have resulted from the oxidation of Fe^{2+} (Yue et al., 2016).

During anoxic storage the Fe^{2+} oxidation rate between 1 and 8 h after filling increased with time from 0.12(±0.01) mg/L/h on the first day to 0.17(±0.02) mg/L/h on day 30. This is probably due to bacterial growth since it is known that at low DO concentrations, biological Fe^{2+} oxidation is faster than abiotic oxidation (Vollrath et al., 2012). In

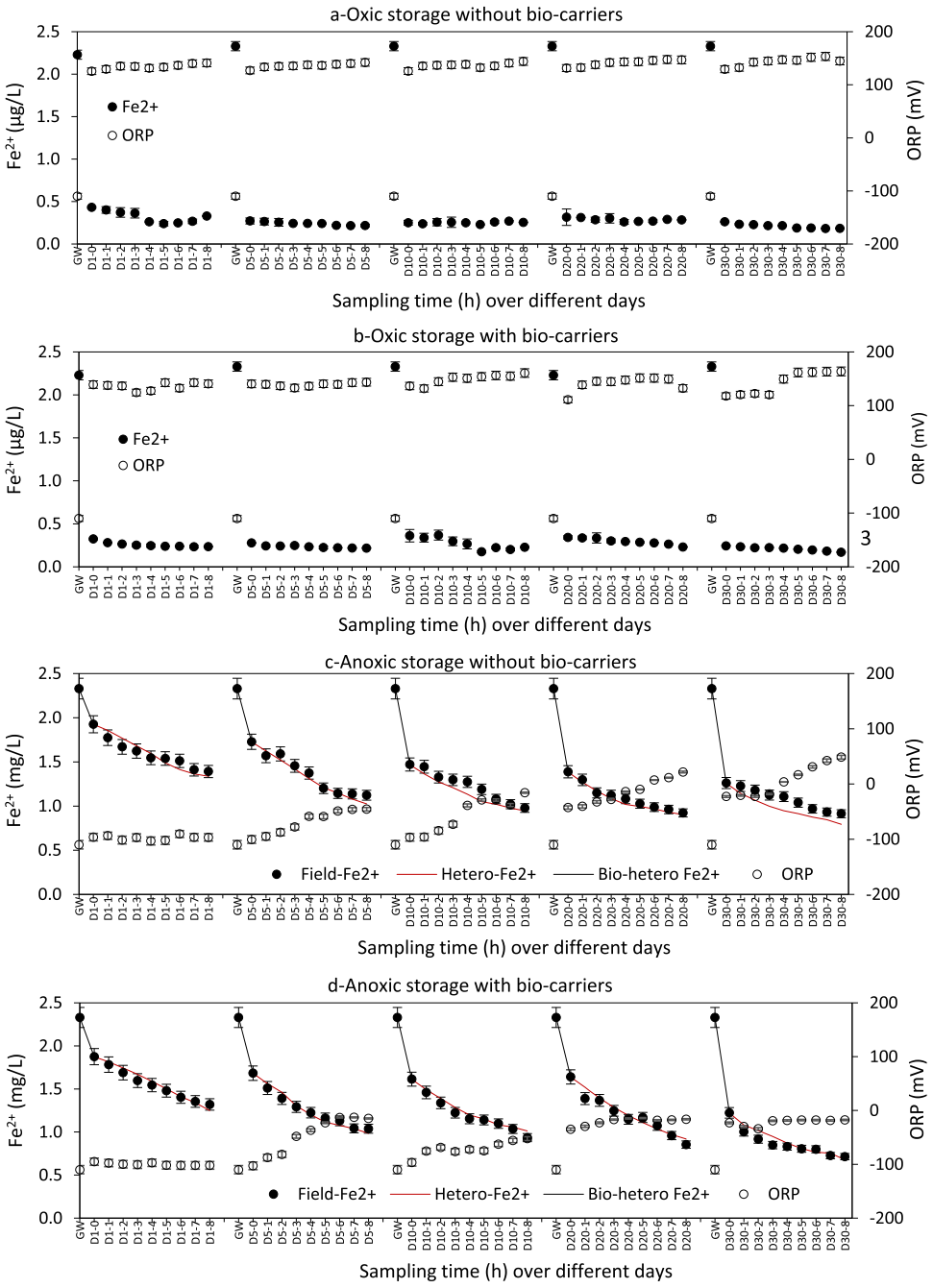

Fig. 4. ORP and Fe^{2+} variation over the experimental periods for oxic storage containers (a) without and (b) with bio-carriers; and anoxic storage containers (c) without and (d) with bio-carriers. The error bars represent the standard deviations.

addition, the oxidation rate upon filling (during the first 10 min) increased as well, potentially explained by Fe^{2+}/Fe-(hydro)oxide and biofilm enhanced surface-related Fe^{2+} oxidation (Tian et al., 2017; van Beek et al., 2015). The combination of heterogeneous and biological Fe^{2+} oxidation led to an overall drop in Fe^{2+} concentration during anoxic storage to an average of 0.94(±0.05) mg/L on day 30 after 8 h, from 1.39(±0.1) mg/L on the first day.

3.4. *Effect of long-term operation on As(III) oxidation and removal*

Arsenic speciation over the 30 experimental days in the oxic and anoxic storage containers without bio-carriers are depicted in Fig. 5, and the results for the bio-carriers containing containers are detailed in Fig. S4. The As(III) oxidation during oxic storage was considerably higher after 30 days than during anoxic storage. During oxic storage in the containers with bio-carriers, the remaining As(III) concentration decreased from 97 µg/L on day 1 to 64 µg/L on day 30. The detected As (III) oxidation rate (13±5 µg/L/h) during oxic storage at day 30 might have resulted from the high DO concentration (Shumlas et al., 2016) and the favorable high pH (7.5) (Wan et al., 2011). In addition, the growth of As(III) oxidizing bacteria over the days in the containers could also have contributed to the increased As(III) oxidation (Ghosh et al., 2018). The removal of As after the first 8 h on day 1 was 54(±5) µg/L, which increased to 100(±10) µg/L at day 5 and remained constant afterward. This higher and constant As removal from day 5 onwards, was possibly caused by the accumulation of HFO flocs (Annaduzzaman et al., 2021).

During anoxic storage, the As(III) oxidation rate also remained nearly stable throughout the 30-day experimentation (Fig. 5b). The

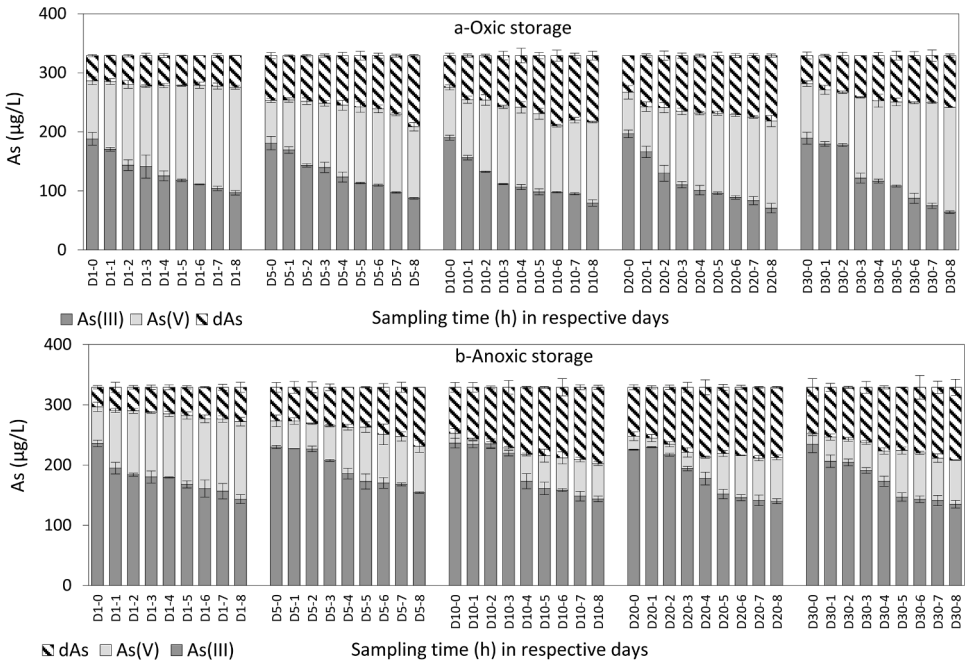

Fig. 5. Oxidation of As(III) and removal over the experimental time at respective days for the (a) oxic, and (b) anoxic storage containers without bio-carriers. The error bars represent the standard deviations.

oxidation of As(III) was most likely due to the continuous Fe^{2+} oxidation over time. The removal of produced As(V) was more effective during anoxic storage compared to oxic storage, and further improved over the 30 experimental days. The As removal per gram of oxidized Fe increased from 61(±5) µg of As on day 1 to 80(±10) µg of As on day 30 during anoxic storage, where during oxic storage the maximum 45(±5) µg of As removal was achieved after 30 days. Apart from the continuous *in-situ* HFO flocs formation and the favorable low pH (6.7) for As(V) adsorption (Klas and Kirk, 2013; Wan et al., 2011) in anoxic storage, both the oxic and anoxic storage containers that contained bio-carriers showed 20 (±5) µg/L higher As(III) oxidation and 17(±5) µg/L higher As removal, respectively, (Fig. S4) compared to the containers without bio-carriers over the experimental period of 30 days, indicating biotic influences, as further discussed below.

3.5. Effect of long term operation on NH_4^+, NO_3^-, and PO_4^{3-} concentration

The groundwater NH_4^+, NO_3^-, and PO_4^{3-} concentrations were on average 0.96 mg/L, 0.39 mg/L, and 2.15 mg/L, respectively (Table 1). During both oxic and anoxic storage, oxidation of NH_4^+ was observed after 10 days (Fig. 6a). The decrease in NH_4^+ concentration during oxic storage resulted from the commencement of biological ammonium oxidation (Koch et al., 2019; van Kessel et al., 2015), leading to an increasing NO_3^- concentration from 0.25±0.1 mg/L to 0.73(±0.10) mg/L. However, during anoxic storage without bio-carriers, the NH_4^+ concentration decreased with only 0.15(±0.05) mg/L (Fig. 6a) over the entire experimental 30 days, where the concentration of NO_3^- after 10 days increased from 0.25(±0.05) mg/L to 0.80(±0.05) mg/L (Fig. 6b). Both the bio-carriers containing containers (oxic and anoxic) showed a ±5% higher decrease in NH_4^+ concentrations which resulted in ±9% elevated NO_3^- formation (Fig. S5a,b) compared to the containers without bio-carriers. The nitrification process, although starting-up slowly, was not hindered by the slow/partial Fe^{2+} oxidation in the anoxic containers.

The concentrations of PO_4^{3-} dropped drastically during oxic storages: from its source groundwater concentration of 2.15 mg/L to an average of 0.65(±0.05) mg/L (Fig. 6c). This decrease in PO_4^{3-} concentration during oxic storage with and without bio-carriers, compared to anoxic storage, justified its removal with HFO flocs originated from rapid (2.03 mg/L) Fe^{2+} oxidation (Fig. 4a). Over 8 h of observation, the PO_4^{3-} removal remained constant (±3%), likely due to the lack of new HFO floc formation. However, during anoxic storage the PO_4^{3-} removal followed the slow/step-wise Fe^{2+} oxidation and removal process (Annaduzzaman et al., 2021): over 30 days and after 8 h PO_4^{3-} decreased from an initial concentration of 2.03(±0.05) mg/L to an average of 1.2(±0.19) mg/L, where Fe^{2+} concentration decreased from an initial concentration of 1.88(±0.1) mg/L to 1.66(±0.14) mg/L.

3.6. Microbial communities in the container's biomass

The metagenomics analysis of the microbial community from the oxic and anoxic container walls showed the presence of various microbial activities. A predominance of Gram-negative bacteria family, specifically Proteobacteria groups such as *Comamonadaceae, Hydrogenophilaceae, Rhodocyclaceae* was observed (Fig. S6). Gram-negatives are usually dominant in water bodies, especially in the subterrestrial systems and such predominance has been reported in other studies from the Ganges-Brahmaputra-Meghna Delta region before (Chakraborty et al., 2020; Ghosh et al., 2014). Germination of spores and abundance of Gram positives (such as *Geodermatophilaceae, Actinopolysporaceae, Saccharopolyspora, Bacillus, Aeromicrobium, Oceanobacillus*) were found on the walls of containers with oxic water only.

The metagenomic library datasets from the oxic storage containers (S1, S2, S3) and anoxic storage containers (S1, S2, S3) were clustered and are presented in Fig. 7. In the oxic storage containers, after an incubation period of 30 days, the presence of the bacterial species *Pseudorhodoferrax, Thiobacter, Sideroxydans, Gallionella, Patulibacter, Pedomicrobium, Tepidicella,* and *Acidibacillus* were observed. These bacteria are known to accelerate Fe^{2+} oxidation (Meijler et al., 2002). However, no or limitedly available Fe^{2+} in the oxic storage containers does not imply the notion that these bacteria were involved in Fe^{2+} oxidation only.

In the anoxic storage containers, different chemolithotrophic Fe^{2+} oxidizing bacterial genus was found except for *Pseudorhodoferrax,* which was available in both the oxic and anoxic storage containers. The identified possible chemolithotrophic Fe^{2+}-oxidizers in the anoxic

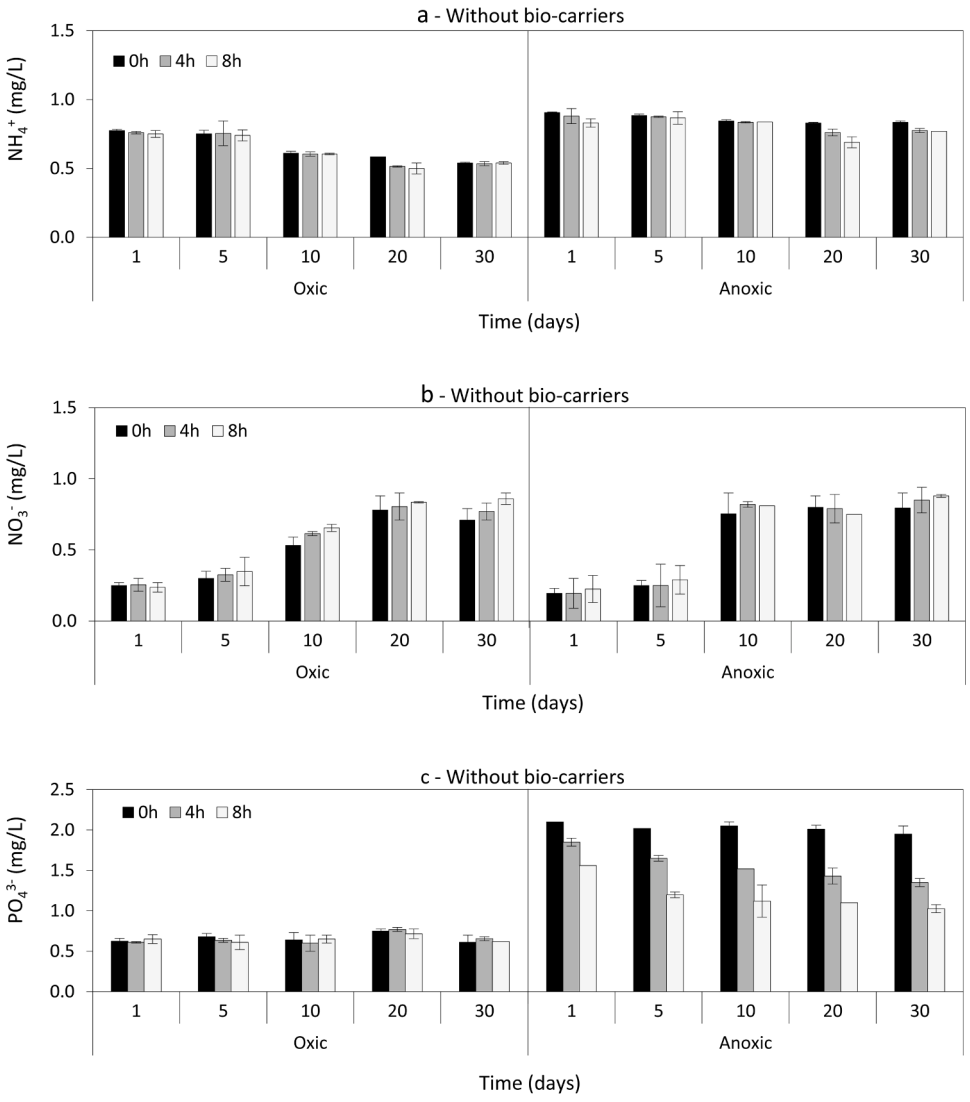

Fig. 6. The concentration of (a) NH_4^+; (b) NO_3^- and (c) PO_4^{3-} at different sampling times (1, 4, and 8 h) over the experimental period of 30 days of the oxic and anoxic storage containers in the absence of bio-carriers. The error bars represent the standard deviations.

storage containers were *Nitrosomonas, Rhodobacter, and Sphingobacterium* (Table S2). Besides Fe^{2+} oxidation and flocculation, the abundance of Fe-oxidizers along with thiosulfate oxidizers like *Thermithiobacillus, Paucimonas, Thiobacillus, Dyella, Acidibacillus* might also lead to acidification and lowering of pH (Fisher et al., 2008; Ilgrande et al., 2018). This pH decreases further supported a higher As removal by adsorption with the freshly formed HFO flocs in the anoxic storage container.

The absence of the As(III) oxidizing bacterial genus in the anoxic storage containers indicated that the observed As(III) oxidation was probably controlled by continuous and slow/step-wise Fe^{2+} oxidation. However, the observed stable As(III) oxidation during oxic conditions might have been associated with detected *aioA* gene expression of the As (III) oxidizing bacterial groups (Fig. 7), such as - *Sideroxydans, Gallionella, Hydrogenophaga* (de Vet et al., 2011; Ghosh et al., 2018). In addition, the bacterial population on the wall of the container under anoxic conditions was characterized by a higher abundance of *Nitrospirae*, (*Nitrospiraceae*) compared to oxic conditions (Fig. 7), suggesting a possible enhancement of nitrification (Bryce et al., 2018; Koch et al., 2019). Furthermore, the presence of ammonia-oxidizing groups like *Nitrosomonas, Chitinivorax, Legionella, Brevibacterium*, and the absence of nitrite oxidoreductase producing bacterial groups like *Nitrobacter*, may result in possible nitrite (intermediate NO_2^-) production (Ilgrande et al., 2018). The NO_3^- production from NH_4^+ could also attribute to the high rate of nitrate reduction coupled (*Massilia, Candidatus, Paracoccus, Pseudorhodoferrax, Comamonadceae, Hydrogenophaga, Methylomonas*) with dissimilatory Fe^{2+} oxide reduction in the storage containers (Shaw et al., 2020). Overall, the microbial processes fortify additional As removal during the incubation and slow oxidation period in the anoxic storage containers.

4. Conclusions

The conventional practice of aeration before storage, where rapid and complete Fe^{2+} oxidation takes place, results in poor As removal despite the presence of sufficient native-Fe^{2+} in the source water. The current study hypothesized that the novel concept of anoxic storage will delay the groundwater native-Fe^{2+} oxidation, and consequently, the *in-situ* HFO flocs formation would allow for higher As sorption per unit Fe in opposition to the conventional oxic storage. The oxic and anoxic storage container experiments were conducted in pilot scale in the presence and absence of bio-carriers, over 30 days with natural groundwater containing Fe^{2+} (2.33 mg/L), As (>300 μg/L), and other contaminants like PO_4^{3-} (2.15 mg/L) and NH_4^+ (0.96 mg/L). It was found that application of anoxic storage enhanced As removal from groundwater, containing ≥300 μg/L of As and 2.33 mg/L of Fe^{2+}, in Rajshahi, Bangladesh. Although the oxidation of Fe^{2+} and As(III) during oxic

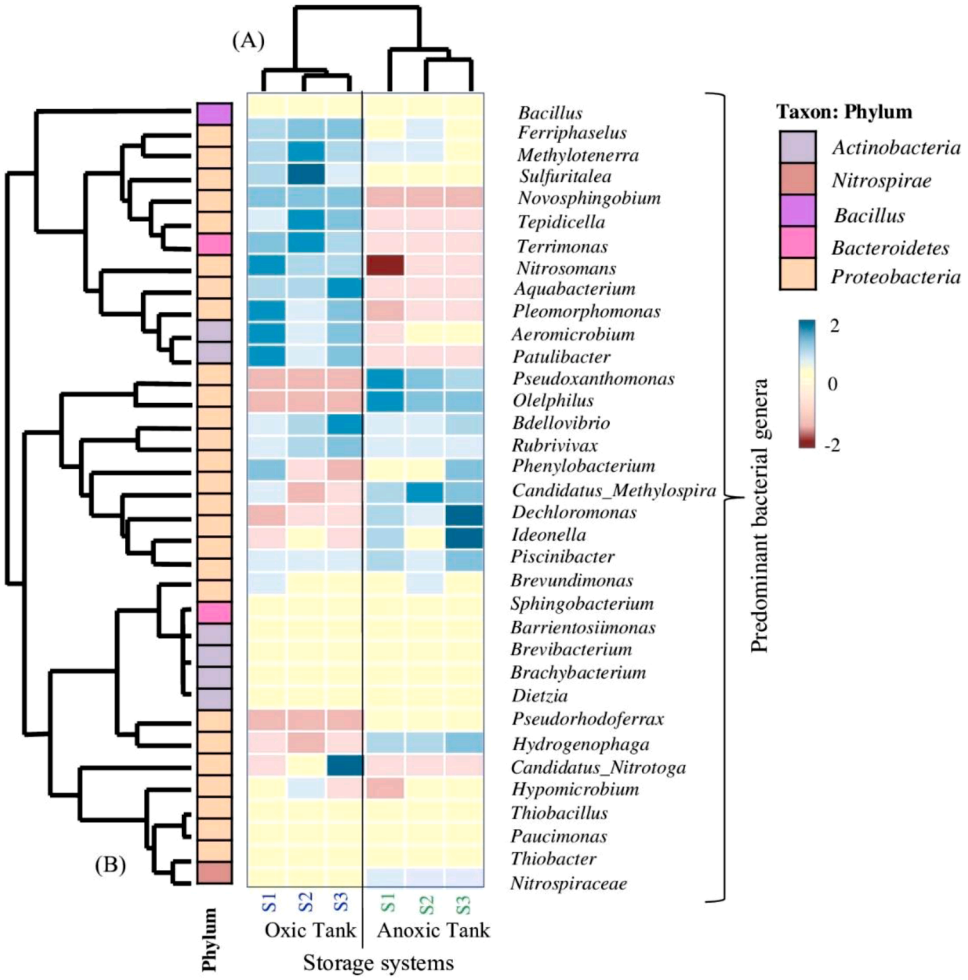

Fig. 7. (A) The samples for generating the metagenomic libraries are clustered based on Weighted Unifrac distance in a UPGMA cluster tree. (B) The predominant common 35 bacterial genera were used to generate a taxonomic heat map and understand their distribution in different storage container setups, where the gradient indicates the distance between the raw score and the mean of the standard deviation. Samples from the oxic storage containers are represented in blue and from the anoxic storage containers are represented in green.

storage was considerably faster, the As/Fe removal ratio was higher during anoxic storage (61−80±5 μgAs/mgFe) compared to the oxic storage (45±5 μgAs/mgFe). This higher As removal efficacy could not be attributed to the speciation of As, since As(V) concentrations were higher during oxic storage, due to more favorable abiotic (As(III) oxidation by O_2 and Fenton-like intermediates) and biotic (As(III) oxidizing bacteria, e.g., *Sideroxydans, Gallionella, Hydrogenophaga)* conditions. The bio-carriers containing storage containers (oxic and anoxic) improved only ±20% of As oxidation and removal compared to the without bio-carriers containing storage containers. Therefore, the improved performance in the anoxic containers was likely as a consequence of the continuous, in-situ hydrous ferric oxide floc formation in this flow-through system, as well as the favorable lower pH (6.9) aiding higher sorption capacities for the gradually formed As(V).

Declaration of Competing Interest

The authors declare that they have no known competing financial interests or personal relationships that could have appeared to influence the work reported in this paper.

Acknowledgments

This study was supported by the NWO-WOTRO funded DELTAP project. All the research assistants from RUET, Rajshahi University, and EPRC are highly acknowledged for their support during the experimentation in Rajshahi, Bangladesh. The authors also thank the landowner Md Sirajul Islam, and his family, without their support, this work would not be possible as the work required to stay for the whole day over the entire experimental period. Finally, the authors are thankful to Nadia van Pelt for her invaluable help with English grammar revision.

Supplementary materials

Supplementary material associated with this article can be found, in the online version, at doi:10.1016/j.watres.2021.117404.

References

Amstaetter, K., Borch, T., Larese-Casanova, P., Kappler, A., 2010. Redox transformation of arsenic by Fe(II)-activated Goethite (α-FeOOH). Environ. Sci. Technol. 44, 102–108. https://doi.org/10.1021/es901274s.

Andrews, S., Gilley, J., Coleman, M.P., 2010. Difference tracker: imageJ plugins for fully automated analysis of multiple axonal transport parameters. J. Neurosci. Methods. 193, 281–287. https://doi.org/10.1016/j.jneumeth.2010.09.007.

Annaduzzaman, M., Rietveld, L.C., Hoque, B.A., Bari, M.N., van Halem, D., 2021. Arsenic removal from iron-containing groundwater by delayed aeration in dual-media sand filters. J. Hazard. Mater. 411, 124823 https://doi.org/10.1016/j.jhazmat.2020.124823.

Bai, Y., Chang, Y., Liang, J., Chen, C., Qu, J., 2016. Treatment of groundwater containing Mn(II), Fe(II), As(III) and Sb(III) by bioaugmented quartz-sand filters. Water Res. 106, 126–134. https://doi.org/10.1016/j.watres.2016.09.040.

Begum, S.A., Golam Hyder, A.H.M., Vahdat, N., 2016. Adsorption isotherm and kinetic studies of As(V) removal from aqueous solution using cattle bone char. J. Water Supply 65, 244–252. https://doi.org/10.2166/aqua.2016.089.

Bissen, M., Frimmel, F.H., 2003. Arsenic - a review. Part II: oxidation of arsenic and its removal in water treatment. Acta Hydrochim. Hydrobiol. 31, 97–107. https://doi.org/10.1002/aheh.200300485.

Bruins, J.H., Vries, D., Petrusevski, B., Slokar, Y.M., Kennedy, M.D., 2014. Assessment of manganese removal from over 100 groundwater treatment plants. J. Water Supply 63, 268–280. https://doi.org/10.2166/aqua.2013.086.

Bryce, C., Blackwell, N., Schmidt, C., Otte, J., Huang, Y.M., Kleindienst, S., Tomaszewski, E., Schad, M., Warter, V., Peng, C., Byrne, J.M., Kappler, A., 2018. Microbial anaerobic Fe(II) oxidation – ecology, mechanisms and environmental implications. Environ. Microbiol. 20, 3462–3483. https://doi.org/10.1111/1462-2920.14328.

Caporaso, J.G., Bittinger, K., Bushman, F.D., DeSantis, T.Z., Andersen, G.L., Knight, R., 2010. PyNAST: a flexible tool for aligning sequences to a template alignment. Bioinformatics 26, 266–267. https://doi.org/10.1093/bioinformatics/btp636.

Casentini, B., Falcione, F.T., Amalfitano, S., Fazi, S., Rossetti, S., 2016. Arsenic removal by discontinuous ZVI two steps system for drinking water production at household scale. Water Res. 106 https://doi.org/10.1016/j.watres.2016.09.057.

Chakraborty, A., DasGupta, C.K., Bhadury, P., 2020. Diversity of Betaproteobacteria revealed by novel primers suggests their role in arsenic cycling. Heliyon 6, e03089. https://doi.org/10.1016/j.heliyon.2019.e03089.

Chakraborty, M., Mukherjee, A., Ahmed, K.M., 2015. A review of groundwater arsenic in the Bengal Basin, Bangladesh and India : from source to sink. Current Pollut. Rep. 1, 220–247. https://doi.org/10.1007/s40726-015-0022-0.

Chakraborty, T.K., Ghosh, P., Jahan, S., Ghosh, G.C., 2016. Performance evaluation of existing community level arsenic removal plants for arsenic free drinking water supply in Jessore and Jhenidah Districts of Bangladesh. Am. J. Environ. Protect. 5, 115–120. https://doi.org/10.11648/j.ajep.20160505.12 https://doi.org/doi:

Ciardelli, M.C., Xu, H., Sahai, N., 2008. Role of Fe(II), phosphate, silicate, sulfate, and carbonate in arsenic uptake by coprecipitation in synthetic and natural groundwater. Water Res. 42, 615–624. https://doi.org/10.1016/j.watres.2007.08.011.

Crognale, S., Casentini, B., Amalfitano, S., Fazi, S., Petruccioli, M., Rossetti, S., 2019. Biological As(III) oxidation in biofilters by using native groundwater microorganisms. Sci. Total Environ. 651, 93–102. https://doi.org/10.1016/j.scitotenv.2018.09.176.

Cui, J., Du, J., Tian, H., Chan, T., Jing, C., 2018. Rethinking anaerobic As(III) oxidation in filters: effect of indigenous nitrate respirers. Chemosphere 196, 223–230. https://doi.org/10.1016/j.chemosphere.2017.12.158.

de Vet, W.W.J.M., Dinkla, I.J.T., Rietveld, L.C., van Loosdrecht, M.C.M., 2011. Biological iron oxidation by *Gallionella* spp. in drinking water production under fully aerated conditions. Water Res. 45, 5389–5398. https://doi.org/10.1016/j.watres.2011.07.028.

Dixit, S., Hering, J.G., 2003. Comparison of arsenic(V) and arsenic(III) sorption onto iron oxide minerals: implications for arsenic mobility. Environ. Sci. Technol. 37, 4182–4189. https://doi.org/10.1021/es030309t.

Farmer, J.G., Johnson, L.R., Farmer, J.G., Johnson, L.R., 1990. Assessment of occupational exposure to inorganic arsenic based on urinary concentrations and speciation of arsenic. British Journal of Industrial Medicine 47, 342–348. https://doi.org/10.1136/oem.47.5.342.

Fisher, J.C., Wallschläger, D., Planer-Friedrich, B., Hollibaugh, J.T., 2008. A new role for sulfur in arsenic cycling. Environ. Sci. Technol. 42, 81–85. https://doi.org/10.1021/es0713936.

Ghosh, D., Bhadury, P., Routh, J., 2018. Coping with arsenic stress: adaptations of arsenite-oxidizing bacterial membrane lipids to increasing arsenic levels. MicrobiologyOpen 7, e00594. https://doi.org/10.1002/mbo3.594.

Ghosh, D., Bhadury, P., Routh, J., 2014. Diversity of arsenite oxidizing bacterial communities in arsenic-rich deltaic aquifers in West Bengal, India. Front. Microbiol. 5, 1–14. https://doi.org/10.3389/fmicb.2014.00602.

Gude, J.C.J., Joris, K., Huysman, K., Rietveld, L.C., van Halem, D., 2018a. Effect of supernatant water level on As removal in biological rapid sand filters. Water Res. X 1, 100013. https://doi.org/10.1016/j.wroa.2018.100013.

Gude, J.C.J., Rietveld, L.C., van Halem, D., 2018b. As(III) removal in rapid filters: effect of pH, Fe(II)/Fe(III), filtration velocity and media size. Water Res. 147, 342–349. https://doi.org/10.1016/j.watres.2018.10.005.

Gude, J.C.J., Rietveld, L.C., van Halem, D., 2016. Fate of low arsenic concentrations during full-scale aeration and rapid filtration. Water Res. 88, 566–574. https://doi.org/10.1016/j.watres.2015.10.034.

Guo, H., Ren, Y., Liu, Q., Zhao, K., Li, Y, 2013. Enhancement of arsenic adsorption during mineral transformation from siderite to goethite: Mechanism and application. Environ. Sci. Technol. 47, 1009–1016. https://doi.org/10.1021/es303503m.

Han, X., Song, J., Li, Y.L., Jia, S.Y., Wang, W.-H., Huang, F.-G., Wu, S.-H., 2016. As(III) removal and speciation of Fe (Oxyhydr)oxides during simultaneous oxidation of As (III) and Fe(II). Chemosphere 147, 337–344. https://doi.org/10.1016/j.chemosphere.2015.12.128.

Hug, S.J., Canonica, L., Wegelin, M., Gechter, D., von Gunten, U., 2001. Solar oxidation and removal of arsenic at circumneutral pH in iron containing waters. Environ. Sci. Technol. 35, 2114–2121. https://doi.org/10.1021/es001551s.

Hug, S.J., Leupin, O., 2003. Iron-catalyzed oxidation of Arsenic(III) by oxygen and by hydrogen peroxide: pH-dependent formation of oxidants in the Fenton reaction. Environ. Sci. Technol. 37, 2734–2742. https://doi.org/10.1021/es026208x.

Ilgrande, C., Leroy, B., Wattiez, R., Vlaeminck, S.E., Boon, N., Clauwaert, P., 2018. Metabolic and proteomic responses to salinity in synthetic nitrifying communities of *Nitrosomonas* spp. and *Nitrobacter* spp. Front. Microbiol.

Karori, S., Clifford, D., Ghurye, G., Samanta, G., 2006. Development of a field speciation method. Am. Water Works Assoc. 98, 128–141. https://doi.org/10.1002/j.1551-8833.2006.tb07666.x.

Katsoyiannis, I.A., Voegelin, A., Zouboulis, A.I., Hug, S.J., 2015. Enhanced As(III) oxidation and removal by combined use of zero valent iron and hydrogen peroxide in aerated waters at neutral pH values. J. Hazard. Mater. 297, 1–7. https://doi.org/10.1016/j.jhazmat.2015.04.038.

Katsoyiannis, I.A., Zikoudi, A., Hug, S.J., 2008. Arsenic removal from groundwaters containing iron, ammonium, manganese and phosphate: a case study from a treatment unit in northern Greece. Desalination 224, 330–339. https://doi.org/10.1016/j.desal.2007.06.014.

Katsoyiannis, I.A., Zouboulis, A.I., 2004. Application of biological processes for the removal of arsenic from groundwaters. Water Res. 38, 17–26. https://doi.org/10.1016/j.watres.2003.09.011.

Kim, M.J., Nriagu, J., 2000. Oxidation of arsenite in groundwater using ozone and oxygen. Sci. Total Environ. 247, 71–79. https://doi.org/10.1016/S0048-9697(99)00470-2.

Klas, S., Kirk, D.W., 2013. Advantages of low pH and limited oxygenation in arsenite removal from water by zero-valent iron. J. Hazard. Mater. 252–253, 77–82. https://doi.org/10.1016/j.jhazmat.2013.02.044.

Koch, H., van Kessel, M.A.H.J., Lücker, S., 2019. Complete nitrification : insights into the ecophysiology of comammox Nitrospira. Appl. Microbiol. Biotechnol. 103, 177–189.

Lafferty, B.J., Ginder-Vogel, M., Zhu, M., Livi, K.J.T., Sparks, D.L., 2010. Arsenite oxidation by a poorly crystalline manganese-oxide. 2. results from X-ray absorption spectroscopy and X-ray diffraction. Environ. Sci. Technol. 44, 8467–8472. https://doi.org/10.1021/es102016c.

Langille, M.G.I., Zaneveld, J., Caporaso, J.G., McDonald, D., Knights, D., Reyes, J.A., Clemente, J.C., Burkepile, D.E., Vega Thurber, R.L., Knight, R., Beiko, R.G., Huttenhower, C., 2013. Predictive functional profiling of microbial communities using 16S rRNA marker gene sequences. Nat. Biotechnol. 31, 814–821. https://doi.org/10.1038/nbt.2676.

Leupin, O.X., Hug, S.J., 2005. Oxidation and removal of arsenic (III) from aerated groundwater by filtration through sand and zero-valent iron. Water Res. 39, 1729–1740. https://doi.org/10.1016/j.watres.2005.02.012.

Li, L., van Genuchten, C.M., Addy, S.E.A., Yao, J., Gao, N., Gadgil, A.J., 2012. Modeling As(III) Oxidation and Removal with Iron Electrocoagulation in Groundwater. Environ. Sci. Technol. 46, 12038–12045. https://doi.org/10.1021/es302456b.

Lowry, J.D., Lowry, S.B., 2002. Oxidation of As (III) by Aeration and Storage. United States Environment Protection Agency. EPA/600/R-01/102.

Luzi, S., Pham, T.K.T., Pham, H.V., Schertenleib, R., 2004. Household Sand Filters for Arsenic Removal – Technical Report. Swiss Federal Institute for Environmental Science and Technology (EAWAG), Ueberlandstr. 133, CH-8600 Duebendorf, Switzerland.

Meijler, M.M., Arad-Yellin, R., Cabantchik, Z.I., Shanzer, A., 2002. Synthesis and evaluation of iron chelators with masked Hydrophilic Moieties. J. Am. Chem. Soc. 124, 12666–12667. https://doi.org/10.1021/ja027013s.

Mercer, K.L., Tobiason, J.E., 2008. Removal of arsenic from high ionic strength solutions: effects of ionic strength, pH, and preformed versus in situ formed HFO. Environ. Sci. Technol. 42, 3797–3802. https://doi.org/10.1021/es702946s.

Morgan, B., Lahav, O., 2007. The effect of pH on the kinetics of spontaneous Fe(II) oxidation by O_2 in aqueous solution - basic principles and a simple heuristic description. Chemosphere 68, 2080–2084. https://doi.org/10.1016/j.chemosphere.2007.02.015.

Muyzer, G., de Waal, E.C., Uitterlinden, A.G., 1993. Rapid lipid biomarker analysis for quantitative assessment of microbial community composition and activity. Appl. Environ. Microbiol. Microbiol. 59, 695–700 doi:0099-2240/93/030695-06$02.00/0.

Niazi, N.K., Bibi, I., Shahid, M., Ok, Y.S., Burton, E.D., Wang, H., Shaheen, S.M., Rinklebe, J., Lüttge, A., 2018. Arsenic removal by perilla leaf biochar in aqueous solutions and groundwater: an integrated spectroscopic and microscopic examination. Environ. Pollut. 232, 31–41. https://doi.org/10.1016/j.envpol.2017.09.051.

Nordstrom, D.K., 2002. Worldwide occurrences of arsenic in groundwater. Science 296, 2143–2145. https://doi.org/10.1126/science.1072375.

Pio, I., Scarlino, A., Bloise, E., Mele, G., Santoro, O., Pastore, T., Santoro, D., 2015. Efficient removal of low-arsenic concentrations from drinking water by combined coagulation and adsorption processes. Sep. Purif. Technol. 147, 284–291. https://doi.org/10.1016/j.seppur.2015.05.002.

Roberts, L.C., Hug, S.J., Ruettimann, T., Billah, M., Khan, A.W., Rahman, M.T., 2004. Arsenic removal with Iron(II) and Iron(III) in waters with high silicate and phosphate concentrations. Environ. Sci. Technol. 38, 307–315. https://doi.org/10.1021/es0343205.

Senn, A.C., Hug, S.J., Kaegi, R., Hering, J.G., Voegelin, A., 2018. Arsenate co-precipitation with Fe(II) oxidation products and retention or release during precipitate aging. Water Res. 131, 334–345. https://doi.org/10.1016/j.watres.2017.12.038.

Shafiquzzaman, M., Azam, M.S., Nakajima, J., Bari, Q.H., 2011. Investigation of arsenic removal performance by a simple iron removal ceramic filter in rural households of Bangladesh. Desalination 265, 60–66. https://doi.org/10.1016/j.desal.2010.07.031.

Shaw, D.R., Ali, M., Katuri, K.P., Gralnick, J.A., Reimann, J., Mesman, R., van Niftrik, L., Jetten, M.S.M., Saikaly, P.E., 2020. Extracellular electron transfer-dependent anaerobic oxidation of ammonium by anammox bacteria. Nat Commun 11, 2058. https://doi.org/10.1038/s41467-020-16016-y.

Shumlas, S.L., Singireddy, S., Thenuwara, A.C., Attanayake, N.H., Reeder, R.J., Strongin, D.R., 2016. Oxidation of arsenite to arsenate on birnessite in the presence of light. Geochem. Trans. 17, 1–10. https://doi.org/10.1186/s12932-016-0037-5.

Smedley, P.L., Kinniburgh, D.G., 2002. A review of the source, behaviour and distribution of arsenic in natural waters. Appl. Geochem. 17, 517–568. https://doi.org/10.1016/S0883-2927(02)00018-5.

Sorlini, S., Gialdini, F., 2010. Conventional oxidation treatments for the removal of arsenic with chlorine dioxide, hypochlorite, potassium permanganate and monochloramine. Water Res. 44, 5653–5659. https://doi.org/10.1016/j.watres.2010.06.032.

Stumm, W., Lee, G.F., 1961. Oxygenation of ferrous iron. Ind. Eng. Chem. 53, 143–146. https://doi.org/10.1021/ie50614a030.

Tian, Z., Feng, Y., Guan, Y., Shao, B., Zhang, Y., Wu, D., 2017. Opposite effects of dissolved oxygen on the removal of As(III) and As(V) by carbonate structural Fe(II). Sci. Rep. 7, 1–11. https://doi.org/10.1038/s41598-017-17108-4.

van Beek, C.G.E.M., Dusseldorp, J., Joris, K., Huysman, K., Leijssen, H., Schoonenberg Kegel, F., de Vet, W.W.J.M., van De Wetering, S., Hofs, B., 2015. Contributions of homogeneous, heterogeneous and biological iron(II) oxidation in aeration and rapid sand filtration (RSF) in field sites. J. Water Supply 65, 195–207. https://doi.org/10.2166/aqua.2015.059.

van Kessel, M.A.H.J., Speth, D.R., Albertsen, M., Nielsen, P.H., den Camp, H.J.M.O., Kartal, B., Jetten, M.S.M., Lücker, S., 2015. Complete nitrification by a single microorganism. Nature 528, 555–559. https://doi.org/10.1038/nature16459.

Villalobos, M., Escobar-Quiroz, I.N., Salazar-Camacho, C., 2014. The influence of particle size and structure on the sorption and oxidation behavior of birnessite: I. Adsorption of As(V) and oxidation of As(III). Geochim. Cosmochim. Acta 125, 564–581. https://doi.org/10.1016/j.gca.2013.10.029.

Vollrath, S., Behrends, T., Van Cappellen, P., 2012. Oxygen dependency of neutrophilic Fe(II) oxidation by Leptothrix differs from abiotic reaction. Geomicrobiol. J. 29, 550–560. https://doi.org/10.1080/01490451.2011.594147.

Vries, D., Bertelkamp, C., Schoonenberg Kegel, F., Hofs, B., Dusseldorp, J., Bruins, J.H., de Vet, W., van den Akker, B., 2017. Iron and manganese removal: recent advances in modelling treatment efficiency by rapid sand filtration. Water Res. 109, 35–45. https://doi.org/10.1016/j.watres.2016.11.032.

Wan, W., Pepping, T.J., Banerji, T., Chaudhari, S., Giammar, D.E., 2011. Effects of water chemistry on arsenic removal from drinking water by electrocoagulation. Water Res. 45, 384–392. https://doi.org/10.1016/j.watres.2010.08.016.

Wang, L., Giammar, D.E., 2015. Effects of pH, dissolved oxygen, and aqueous ferrous iron on the adsorption of arsenic to lepidocrocite. J. Colloid Interface Sci. 448, 331–338. https://doi.org/10.1016/j.jcis.2015.02.047.

Wang, Z., Bush, R.T., Liu, J., 2013. Arsenic (III) and iron (II) co-oxidation by oxygen and hydrogen peroxide : divergent reactions in the presence of organic ligands. Chemosphere 93, 1936–1941. https://doi.org/10.1016/j.chemosphere.2013.06.076.

WHO, 2011. Arsenic in Drinking-water. World Health Organization.

Yue, G., Guezennec, A.G., Asselin, E., 2016. Extended validation of an expression to predict ORP and iron chemistry: application to complex solutions generated during the acidic leaching or bioleaching of printed circuit boards. Hydrometallurgy 164, 334–342. https://doi.org/10.1016/j.hydromet.2016.06.027.

Zhang, S., Niu, H., Cai, Y., Zhao, X., Shi, Y., 2010. Arsenite and arsenate adsorption on coprecipitated bimetal oxide magnetic nanomaterials: mnFe2O4 and CoFe2O4. Chem. Eng. J. 158, 599–607. https://doi.org/10.1016/j.cej.2010.02.013.